

SAIF: A Sparse Autoencoder Framework for Interpreting and Steering Instruction Following of Language Models

Zirui He^{1,*}, Haiyan Zhao^{1,*}, Yiran Qiao², Fan Yang³,
Ali Payani⁴, Jing Ma², Mengnan Du¹

¹NJIT ²Case Western Reserve University ³Wake Forest University ⁴Cisco

*Equal contribution

{zh296,hz54,mengnan.du}@njit.edu, {yxq350,jxm1384}@case.edu, yangfan@wfu.edu, apayani@cisco.com

Abstract

The ability of large language models (LLMs) to follow instructions is crucial for their practical applications, yet the underlying mechanisms remain poorly understood. This paper presents a novel framework that leverages sparse autoencoders (SAE) to interpret how instruction following works in these models. We demonstrate how the features we identify can effectively steer model outputs to align with given instructions. Through analysis of SAE latent activations, we identify specific latents responsible for instruction following behavior. Our findings reveal that instruction following capabilities are encoded by a distinct set of instruction-relevant SAE latents. These latents both show semantic proximity to relevant instructions and demonstrate causal effects on model behavior. Our research highlights several crucial factors for achieving effective steering performance: precise feature identification, the role of final layer, and optimal instruction positioning. Additionally, we demonstrate that our methodology scales effectively across SAEs and LLMs of varying sizes.

1 Introduction

Large language models (LLMs) have demonstrated remarkable capabilities in following instructions, enabling alignment between model outputs and user objectives. These capabilities are typically gained through instruction tuning methods (Ouyang et al., 2022; Wei et al., 2022), including extensive training data and computationally intensive fine-tuning processes. While these approaches effectively control model behavior, the underlying mechanisms by which models process and respond to instructions remain poorly understood. In-depth mechanistic investigations are essential for improving our ability to control models and enhance their instruction-following capability.

Prior research has attempted to understand instructions following from two perspectives:

1) prompting-based; 2) activation-space-based. Among prompting-based studies, the importance of instruction positions has been thoroughly studied (Liu et al., 2024; Ma et al., 2024). For activation-based studies, Stolfo et al. (2024) propose to manipulate model following instructions with representation vector in residual stream. However, both methods ultimately fail to explain the inner workings of how LLMs follow instructions in a fine-grained manner, i.e. the concept level. Specifically, prompting-based approaches provide insights into better prompt formulation strategies to improve instruction following, while activation-space-based methods provide a possible way to implement steering with instruction following rather than explaining how it works.

In this paper, we propose a novel framework SAIF (Sparse Autoencoder steering for Instruction Following) to understand working mechanisms of instruction following at the concept level through the lens of sparse autoencoders (SAEs). First, we develop a robust method to sample instruction-relevant features. Then, we select influential features using designed metrics and further compute steering vectors (see Figure 1a). Furthermore, we measure the effectiveness of these steering vectors through steering tasks (see Figure 1b). Additionally, we examine the extracted features using Neuronpedia (Lin, 2023) to illustrate how semantically relevant the activating text of features is to instructions. We also measure steering performance to demonstrate the effectiveness of extracted features. Through these tools, we gain some intriguing insights regarding the importance of the feature number used in representing instructions, the role of the last layer, the impact of instruction position and model scale. Our main contributions in this work can be summarized as follows:

- We propose SAIF, a framework that interprets instruction following in LLMs at a fine-grained

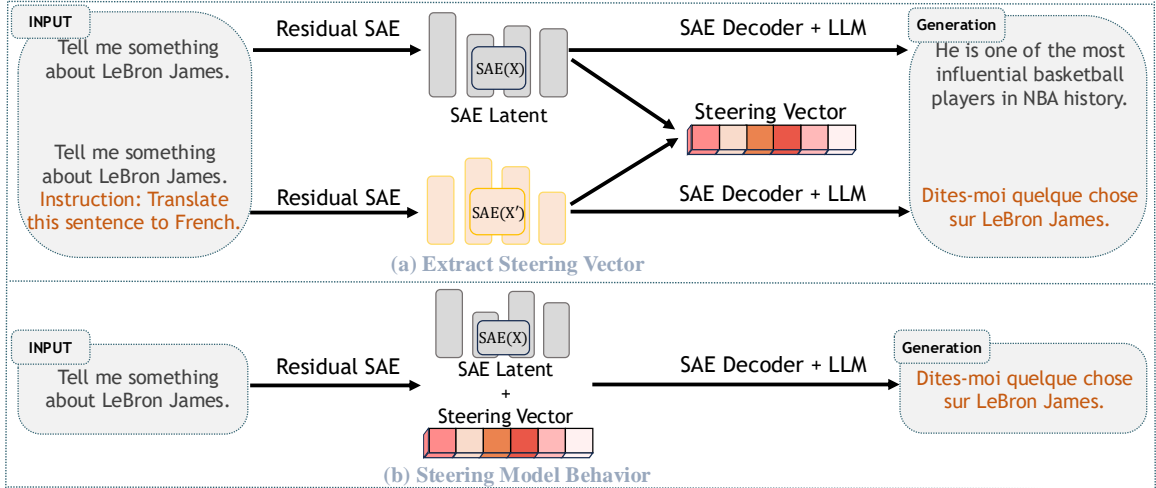


Figure 1: The proposed SAIF framework. The model computes steering vectors from SAE latent differences to guide outputs according to instructions. (a) Extract steering vector. (b) Apply steering for controlled output.

conceptual level. Our analysis reveals how models internally encode and process instructions through interpretable latent features in their representation space.

- We demonstrate that instructions cannot be adequately represented by a single concept in SAEs, but rather comprise multiple high-level concepts. Effective instruction steering requires a set of instruction-relevant features, which our method precisely identifies.
- We reveal the critical role of the last layer in SAE-based activation steering. Moreover, the effectiveness of our framework has been demonstrated across instruction types and model scales.

2 Preliminaries

Sparse Autoencoders (SAEs). Dictionary learning enables disentangling representations into a set of concepts (Olshausen and Field, 1997; Bricken et al., 2023). SAEs are employed to decompose hidden representations into a high-dimension space and then reconstruct the hidden representations. Specifically, the input of SAEs is the hidden representation from a model’s residual stream denoted as $z \in \mathbb{R}^d$ and the reconstructed output is denoted as $\text{SAE}(z) \in \mathbb{R}^d$, we obtain that $z = \text{SAE}(z) + \epsilon$ where ϵ is the error. In our paper, we focus on layer-wise SAEs trained with an encoder $\mathbf{W}_{\text{enc}} \in \mathbb{R}^{d \times m}$ followed by the non-linear activation function, and a decoder $\mathbf{W}_{\text{dec}} \in \mathbb{R}^{m \times d}$ (He et al., 2024). The definition of SAEs is:

$$a(z) = \sigma(z\mathbf{W}_{\text{enc}} + \mathbf{b}_{\text{enc}}), \quad (1)$$

$$\text{SAE}(z) = a(z)\mathbf{W}_{\text{dec}} + \mathbf{b}_{\text{dec}}, \quad (2)$$

where $\mathbf{b}_{\text{enc}} \in \mathbb{R}^m$ and $\mathbf{b}_{\text{dec}} \in \mathbb{R}^d$ are the bias terms. The decomposed high-dimension latent activations $a(z)$ have dimension m and $m \gg d$, which is a highly sparse vector. Note that different SAEs use different non-linear activation function σ . For example, Llama Scope (He et al., 2024) adopts TopK-ReLU, while Gemma Scope (Lieberum et al., 2024) uses JumpReLU (Rajamanoharan et al., 2024).

Steering with SAE Latents. Following Eq. (2), the reconstructed SAE outputs are a linear combination of *SAE latents*, which represent the row vectors of SAE decoder \mathbf{W}_{dec} . The weight of j -th SAE latent is $a(z)_j$. Typically, a prominent dimension $j \in \{1, \dots, m\}$ is chosen, and its decoder latent vector \mathbf{d}_j is scaled with a factor α and then added to the SAE outputs (Ferrando et al., 2025). The computation is as follows:

$$z^{\text{new}} \leftarrow z + \alpha \mathbf{d}_j. \quad (3)$$

This modified representation z^{new} can then be fed back into the model’s residual stream to steer the model’s behavior during generation.

3 Proposed Method

In this section, we introduce the **SAIF**, a framework for analyzing and steering instruction following in LLMs. First, we introduce linguistic variations to construct diverse instruction sentences and related datasets, which are further used to compute SAE latent activations. Second, we develop a two-stage process for computing steering vectors that quantifies the sensitivity of features to instruction presence. Finally, we investigate how these identi-

fied features can be leveraged for steering model behavior, demonstrating a technique for enhancing instruction following while preserving output coherence (see Figure 1).

3.1 Format Instruction Feature

To identify instruction-relevant features given an instruction, we construct a dataset \mathcal{D} with N positive-negative sample pairs. For example, we focus on an instruction `Translate the sentence to`

`French`. In a sample pair, the positive sample refers to a prefix prompt followed by the instruction, while the negative sample refers to the prefix prompt without the instruction sentence.

The *difference-in-means* (Rimsky et al., 2024) is a typical approach to derive concept vectors. It computes the activation differences between each sample pair over the last token, and then averages over all pairs of activation difference vectors. However, directly applying this pipeline to instruction following presents a significant challenge. When a single instruction sentence is used repeatedly to generate samples, the model tends to encode the specific semantic meaning of that instruction rather than learning a general-purpose vector that can reliably execute the intended operation (See Appendix G). Specifically, the derived vector can barely operate the same instruction if we rephrase the instruction in a linguistically different but semantically similar manner. To resolve this challenge, we propose to introduce linguistic variations to extract instruction functions.

We formulate instruction sentences for a given instruction through different strategies. These variations include syntactic reformulations (e.g., imperative to interrogative form, task-oriented to process-based description) and cross-lingual translations (e.g., English, Chinese, German). In this way, we generated six diverse instruction sentences comprehensively capturing key features of an instruction. The instruction design used in our paper is shown in Appendix A.

For each instruction variant, we extract samples’ residual stream representation and compute the corresponding SAE latent activations. While diverse linguistic information are contained, the latent features specifically corresponding to the core instructional concept should maintain relatively consistent activation levels across all variants. These dimensions with consistent activation patterns will be further used to construct instruction vectors.

3.2 Steering Vector Computation

Based on SAE latent activations computed in Section 3.1, we develop a two-step process for computing steering vectors. The first step identifies features that consistently respond to a given instruction, while the second step quantifies their sensitivity.

Given N input samples and a target instruction type (e.g., translation), we first obtain both positive samples (with instruction) and negative samples (without instruction) for each input. For each sample pair i and feature j , we compute the activation state change:

$$\Delta h_{i,j} = \mathbb{1}(h_{i,j}^w > 0) - \mathbb{1}(h_{i,j}^{w/o} > 0), \quad (4)$$

where $h_{i,j}^w$ and $h_{i,j}^{w/o}$ represent the SAE latent activation values with and without instruction respectively, and $\mathbb{1}(\cdot)$ is the indicator function. $\Delta h_{i,j}$ captures whether feature j becomes activated in response to the instruction for sample i . We then compute a sensitivity score C_j for each feature:

$$C_j = \frac{1}{N} \sum_{i=1}^N \mathbb{1}(\Delta h_{i,j} > 0). \quad (5)$$

The score represents the proportion of samples whose feature j becomes activated in response to instructions. Features with higher scores are more consistently responsive to instruction presence. By sorting these sensitivity scores in a descending order, we select the top- k responsive features. These selected features form the instruction-relevant feature set $\mathbf{V} = \{\mathbf{W}_{\text{dec},j} | \text{rank}(C_j) \leq k\}$ where $\mathbf{W}_{\text{dec},j} = \mathbf{W}_{\text{dec}}[j, :]$ denotes the j -th SAE latent. These features will be used for further constructing steering vectors.

3.3 Steering Procedure

Different from the classic steering approach defined in Eq. (3), we hypothesize that instruction following steering requires a set of features to be effective. The individual feature utilized in the classic method focuses on token-level concepts, where individual concepts typically correlate with a few SAE latent activations. As a result, this approach can barely operate instructions. It is partly due to the complexity of sentence-level instructions, which are composed of multiple high-level features represented by a set of SAE latent features. Additionally, SAEs tend to overly split features, which further increases the number of features needed for steering (Ferrando et al., 2025). Thus, we propose

Algorithm 1: The proposed SAIF framework

Input: Input text x ; Target instruction type (e.g., translation, summarization)

Stage 1: Format Instruction Feature

Generate diverse instruction variants

Construct dataset \mathcal{D} with N positive/negative pairs

Stage 2: Compute Steering Vector

for each sample pair i and feature j do

 Compute activation state change:

$$\Delta h_{i,j} = \mathbb{1}(h_{i,j}^w > 0) - \mathbb{1}(h_{i,j}^{w/o} > 0)$$

 Calculate sensitivity score:

$$C_j = \frac{1}{N} \sum_{i=1}^N \mathbb{1}(\Delta h_{i,j} > 0)$$

Sort features by sensitivity scores C_j

Select top- k features as instruction-relevant set \mathbf{V}

Stage 3: Steering Procedure

Obtain residual stream representation z of input x

for each feature $i \in \mathbf{V}$ do

 Compute activation strength: $\alpha_i = \mu_i + \beta s_i$

 where μ_i is mean activation, s_i is std deviation

Apply steering: $z^{new} = z + \sum_{i=1}^k \alpha_i \mathbf{v}_i$

Output: Steered text following the instruction

to determine how to steer with a set of vectors.

Building on top of the feature set \mathbf{V} derived in Section 3.2, we employ the set of features to steer residual stream representation of a certain input at layer l . Our steering is implemented as below:

$$z^{new} = z + \sum_{i=1}^k \alpha_i \mathbf{v}_i, \quad (6)$$

where z represents the residual stream representation of the input over the last token, and α_i denotes the steering strength of feature i . Here, \mathbf{v}_i represents a certain instruction-relevant feature in \mathbf{V} .

As the strength of each selected feature is crucial to steering performance, we further compute the strength of each feature by employing statistical measurements of feature activation values to make it more robust and reliable. The activation strength for feature i is calculated as:

$$\alpha_i = \mu_i + \beta s_i, \quad (7)$$

where μ_i is the mean activation value of feature i observed in instruction-following examples, s_i is the standard deviation of these activation values, and β is a hyperparameter to scale s_i meanwhile controlling the strength value.

4 Experiments

In this section, we conduct experiments to evaluate the effectiveness of SAIF by answering the following research questions (RQs):

- RQ1: How interpretable are the features extracted using SAEs, and do they correspond to

instruction-related concepts? (Section 4.2)

- RQ2: Can the proposed SAIF framework effectively control model behavior? (Section 4.3)
- RQ3: What role does the final Transformer layer play in the instruction following? (Section 4.4)
- RQ4: How does instruction positioning affect the effectiveness of instruction following and feature activation patterns? (Section 4.5)

4.1 Experimental Setup

Datasets and Models. Our experiments are conducted with multiple language models including Gemma-2-2b, Gemma-2-9b (Team et al., 2024) and Llama3.1-8b. The Cross-lingual Natural Language Inference (XNLI) dataset (Conneau et al., 2018) is used to construct input samples. It encompasses diverse languages (including English, French, Spanish, German, Greek, Bulgarian, Russian, Turkish, Arabic, Vietnamese, Thai, Chinese, Hindi, Swahili and Urdu) and rich syntactic structures (such as active/passive voice alternations, negation patterns, and various clause structures). The diverse linguistic patterns within the dataset are essential in constructing a comprehensive set of samples for an instruction. Moreover, it ensures extracting consistent SAE activations from the residual stream of input samples.

Instruction Design. Following the settings in IFEval (Zhou et al., 2023), we investigate three types of instructions: keyword inclusion, summarization, and translation. For keywords inclusion, we provide models with a keyword (e.g., “Sunday”), and expect model output incorporating the specified keyword. For formatting, we instruct the model to perform summarization, where the ideal output should be concise, maintain the key information from the original text, and follow a consistent format with a clear topic sentence followed by supporting details. For translation, we direct the model to translate sentences into different languages (English, French, and Chinese), where the ideal model output should accurately perform the requested translation while preserving the original meaning. The complete set of instructions used for each task is provided in Appendix A.

Implementation Details. We use pre-trained SAEs from Gemma Scope (Lieberum et al., 2024) and Llama Scope (He et al., 2024). When constructing input samples for each instruction, we set the number of positive/negative samples N to 800. For SAE latent extraction, we use sparse au-

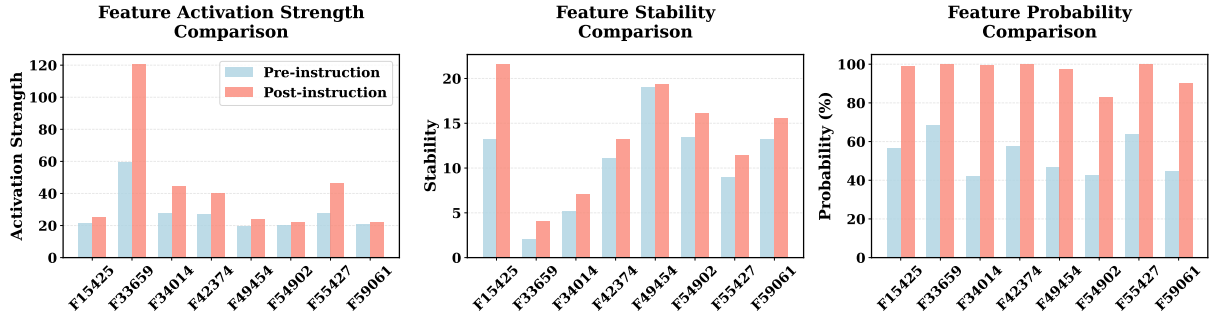


Figure 2: Comparison of feature activation patterns between pre-instruction and post-instruction conditions across different SAE latent dimensions. The plots show three key metrics: activation strength (left), feature stability (middle), and activation probability (right) for eight identified instruction-relevant features.

toencoders with dimensions of 65K and 131K for [Gemma-2-2b-it](#)¹ and [Gemma-2-9b-it](#)² models respectively. We also use SAE with dimension 32K for [Llama3.1-8b](#)³. All experiments were run on 1 NVIDIA A100 GPU. As default settings, for Equation (6), we fix $k = 15$, meaning that we use the top 15 most responsive SAE features for instruction steering. The strategy to choose the optimal k will be further discussed in Section 4.2. For Equation (7), we fix the hyperparameter $\beta = 0$, and we discuss the impact of adjusting this hyperparameter on the steering effect in Appendix C.

SAE Latent Activation Metrics. We consider the following three metrics to quantify features’ behavior and reliability in instruction processing. Note that we only consider features activated on positive samples but not negative samples.

- *Activation Strength*: The mean activation value is calculated as: $\mu_i = \frac{1}{|A_i|} \sum_{a \in A_i} a$, where A_i is the set of non-zero activation values for feature i .
- *Activation Probability*: The probability of feature i is activated across positive/negative samples: $P_i = \frac{|A_i|}{N}$, where N is the total number of positive/negative samples.
- *Activation Stability*: The normalized standard deviation value of non-zero activation values: $\Omega_i = 1/s_i$.

A high-quality instruction-relevant feature should ideally exhibit strong activation (μ_i), consistent triggering (P_i), and stable behavior (Ω_i) across different formulations of the same instruction.

Steering Effectiveness Metrics. We evaluate steering outputs with two metrics: 1) *Strict Ac-*

curacy, which measures the proportion of cases where the model completely follows the instruction, meaning it both understands and produces output exactly as instructed; and 2) *Loose Accuracy*, which measures the proportion of cases where the model partially follows the instruction, meaning it understands the instruction but the output does not fully conform to the requirements. Note that we use GPT-4o-mini to rate the responses, and please refer to the details in Appendix D.

4.2 Analysis of Instruction-Related Concepts

To investigate RQ1, we analyze the interpretability of features extracted using SAEs and assess their correspondence to instruction-related concepts. Our analysis consists of two parts. First, we examine the activating text of extracted features with Neuronpedia (Lin, 2023) to evaluate their semantic relevance to instructions. Second, we compare how strongly the activating examples of top- k features and lower-ranked features correspond to instruction-related concepts, demonstrating the relationship between feature importance and instruction relevance.

We focus on analyzing the consistent instruction-relevant latent activations through the lens of Neuronpedia (Lin, 2023), which provides detailed activated text for each SAE latent. Taking translation-related instructions as an example (e.g., “Translate the sentence to French.”), we identify a notable latent that shows strong activation patterns. This latent exhibits high activation not only for various languages but also for directional prepositions like “to” and “from” that commonly appear in translation instructions, as shown in Table 1. We summarize two key findings as below:

- Our extracted SAE latent features show strong correspondence with instruction-related concepts,

¹<https://huggingface.co/google/gemma-2-2b-it>

²<https://huggingface.co/google/gemma-2-9b-it>

³<https://huggingface.co/meta-llama/Llama-3.1-8B-Instruct>

Table 1: Maximally activating examples for Feature 15425 in Layer 25 of Gemma2-2b-it when prompted with “Translate the sentence to French.” Data sourced from Neuronpedia (Lin, 2023).

Activating Examples with ‘Translate the sentence to French’ (Feature 15425, Layer 25)
The Theory of Super conductivity (1958) (translated from Russian: Consultants Bureau, Inc., New York.
Save your game, go back to change the PS 3 system language settings to English.
We have posted a partial translation of his speech from Yiddish to Hebrew , which was posted in...
I can speak English, but i’m afraid it may be worse than your french.

Table 2: Layer25 Experimental Results

F15453 $k = 1$	F33659 $k = 2$	F65085 $k = 3$	F2369 $k = 13$	F58810 $k = 14$	F21836 $k = 15$
translation	French	language	bienfaits	here	NameInMap
Translation	France	Speaking	attentes	Here	CloseOperation
translators	french	languages	prochaines	Below	Jspwriter

Table 3: Performance of instruction positions, including pre-instruction and post-instruction.

Position	Strict Acc	Loose Acc	Original
Pre-Instruction	0.14	0.47	0.56
Post-Instruction	0.23	0.64	0.75

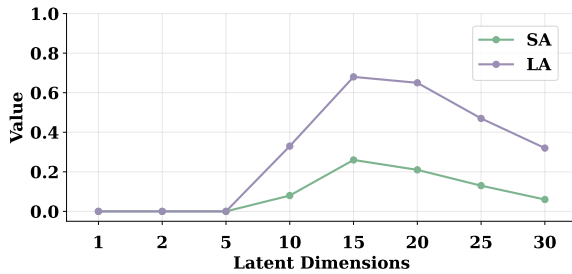


Figure 3: The impact of the number of latent dimensions (k) on our steering experiments. The x-axis represents different values of k , while the y-axis records the accuracy. We track the trend of strict accuracy (SA) and loose accuracy (LA) across 8 different k values.

as demonstrated in Table 1. The extracted features consistently activate on instruction-relevant terms (e.g., “translate”, “French”) and related linguistic elements.

- The activating examples of our extracted top- k features reveal a clear relevance pattern: they are directly corresponding to core instruction elements (e.g., task commands, target specifications), while those of lower-ranked features show decreasing relevance to instruction-relevant terms, capturing more peripheral or contextual information. The result is shown in Table 2. Take the Layer 25 as an example, for the top-13th feature, the top 3 tokens are French words. But for the top-14th and 15th features, the top 3 tokens seem irrelevant to the instruction.

4.3 Steering Performance Analysis

In this section, we evaluate the effectiveness of steering vectors constructed from SAE features and

investigate the optimal number of features needed for reliable control.

Steering Effectiveness. We visualize a case study in Figure 4 and compare the performance of steering results in Figure 5, including both *strict accuracy* and *loose accuracy*. Our analysis reveals several key findings:

- The quantitative results in Figure 5 demonstrate significant improvements in instruction following, with the steered models achieving over 30% strict accuracy across different tasks. The loose accuracy of our steered approach performs nearly on par with prompting-based instruction methods, falling only slightly below. These results strongly indicate that SAIF can effectively extract features for user instructions and adjust LLMs’ behaviors according to relevant instructions.
- The case study in Figure 4 illustrates two distinct scenarios of instruction following: strict adherence (successful Chinese-to-French translation) and loose following (understanding that this is a French translation task). It demonstrates how SAIF manipulates model responses from the failure case toward either strict instruction following or loose instruction following.
- The Gemma-2-9b-it model consistently outperforms Gemma-2-2b-it with slightly higher instruction steering performance across all five tasks, suggesting that SAIF’s effectiveness scales well with model size.
- The LLaMA-3.1-8B model shows comparable performance to the Gemma models across tasks. Looking at French translation as an example, LLaMA-3.1-8B achieves around 30% strict accu-

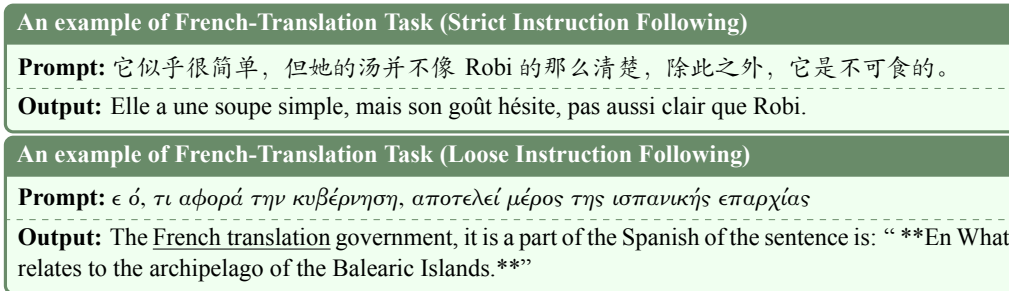


Figure 4: Examples of French translation task outcomes showing strict instruction following and loose instruction following using inputs in different languages. (Gemma-2-2b-it, SAE dimension of 65K)

racy and 65% loose accuracy, which is similar to Gemma-2-2b-it’s performance.

Latent Dimension Analysis. We study the effect of single latent and the number of latents on steering, showing that too few and too many dimensions both lead to failures. For individual latent, we use the single top 1 latent and latent listed in Table 1 for steering. Despite their apparent semantic relevance to translation tasks, the model shows zero accuracy. This suggests that instruction following cannot be captured by a single high-level concept, even when that concept appears highly correlated with specific instruction types.

This observation leads us to investigate whether a combination of multiple latent dimensions could achieve better steering performance. Our experiments, shown in Figure 3, systematically evaluate the impact of varying the number of latent dimensions from 1 to 30. The instructions used here are sourced from French translation task. The results reveal several key patterns:

- Steering performance remains near zero when $k \leq 5$, indicating that too few dimensions are insufficient for capturing instruction-following behavior. Performance begins to improve notably around $k = 10$, with both strict accuracy and loose accuracy showing substantial increases.
- The optimal performance is achieved at $k = 15$, where loose accuracy peaks at approximately 0.7 and strict accuracy reaches about 0.25.
- However, as we increase dimensions beyond $k = 15$, both metrics show a consistent decline. This deterioration becomes more pronounced as k approaches 30, suggesting that excessive dimensions introduce noise that interferes with effective steering.

4.4 The Role of Last Layer Representations in Instruction Processing

In previous sections, we exclusively used SAE from the last Transformer layer for concept vector extraction and instruction steering. In this section, we analyze why extracting concepts and steering from the final layer is most effective.

Concept Extraction Perspective. From the results in Table 4, we observe an intriguing phenomenon that shallower layers are less effective in providing clean instruction-relevant features. Following our default experimental settings, we extract the top 15 SAE features from each layer of the model. The features extracted from the last layer can precisely capture the semantics of ‘French’, showing strong activations on French-related words, where $k = 2$ indicates this feature is considered the second most instruction-relevant feature. Starting from the penultimate layer, as we attempt to trace French-related features, our experimental results reveal that the extracted French-related concepts undergo a gradual shift as the layer depth decreases. Specifically, the feature evolves from exclusively activating on French-related tokens to encompassing a broader spectrum of languages (English, Spanish, Hindi, and Belgian), demonstrating a hierarchical abstraction pattern from language-specific to cross-lingual representations. Moreover, the increasing k values suggest that these French-related features become less instruction-relevant in earlier layers. For Gemma2-2b-it model, before Layer 21, we can no longer identify French-related features among the top 15 SAE features.

Steering Perspective. We conducted steering experiments using the top 15 features extracted from Layers 21-25 respectively under default settings on French Translation task. The results align with our

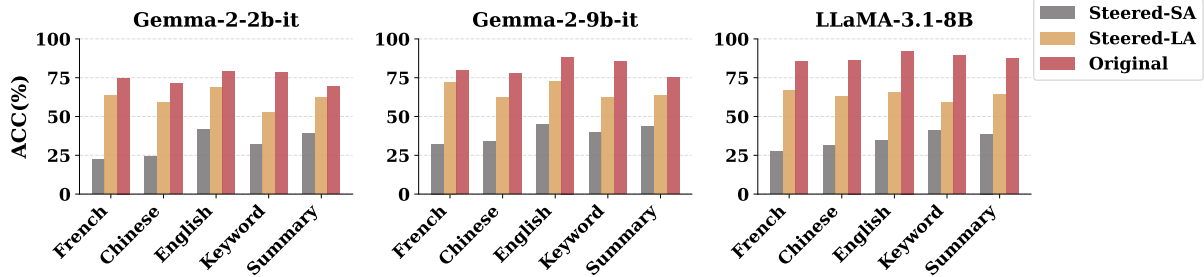


Figure 5: Performance comparison between original model outputs and two steering approaches across different instruction types on Gemma-2-2b-it and Gemma-2-9b-it models. Results show the accuracy percentages for translation tasks (French, Chinese, English), keyword inclusion, and summarization tasks.

Table 4: Analysis of Layer Features

# of Layer	Top 5 tokens with the highest logit increases by the feature influence	# of top_k	# of Feature
25	French, France, french, FRENCH, Paris	2	33659
24	French, nb, french, Erreur, Fonction	8	65238
23	French, France, french, Paris, Francis	15	49043
22	English, english, Spanish, French, Hindi	12	351
21	Belgian, Belgium, Brussels, Flemish, Belgique	14	27665

findings on concept extraction, showing the effectiveness and importance of last layer representation on instruction following. Using loose accuracy as the evaluation metric, we observe that steering with Layer 24 features still maintains some effectiveness, though the loose accuracy drops sharply from 0.64 (Layer 25) to 0.33. Steering attempts using features from earlier layers fail to guide the model towards instruction-following behavior, with the model instead tending to generate repetitive and instruction-irrelevant content.

4.5 Impact of Instruction Position

Previous studies have shown that models’ instruction-following capabilities can vary significantly depending on the relative positioning of instructions and content. This motivates us to examine how instruction positioning affects the activation patterns of previously identified features.

We investigate the effect of instruction position by comparing two patterns: pre-instruction ($P_{pre} = [\text{Instruction}] + [\text{Content}]$) and post-instruction ($P_{post} = [\text{Content}] + [\text{Instruction}]$) as in Liu et al. (2024). Using identical instruction-content pairs while varying only their relative positions allows us to isolate the effects of position. Our analysis reveals several key findings from both the quantitative metrics (see Table 3) and feature activation patterns (see Figure 2):

- Performance metrics demonstrate that post-

instruction positioning consistently outperforms pre-instruction, with post-instruction achieving higher accuracy across all measures (Strict Acc: 0.23 vs 0.14, Loose Acc: 0.64 vs 0.47), aligning with the result in Liu et al. (2024).

- Feature activation patterns show that post-instruction enables more robust processing with stronger activation peaks (particularly for key features like F33659), more consistent stability scores, and higher activation probabilities (>80%) across most features compared to pre-instruction’s more variable patterns.

5 Conclusions

In this paper, we have introduced to use SAEs to analyze instruction following in LLMs, revealing the underlying mechanisms through which models encode and process instructions. Our analysis demonstrates that instruction following is mediated by interpretable latent features in the model’s representation space. We have developed a lightweight steering technique that enhances instruction following by making targeted modifications to specific latent dimensions. We find that effective steering requires the careful combination of multiple latent features with precisely calibrated weights. Extensive experiments across diverse instruction types have demonstrated that our proposed steering approach enables precise control over model behavior while consistently maintaining coherent outputs.

Limitations

One limitation of our steering approach is that it sometimes produces outputs that only partially follow the intended instructions, particularly when handling complex tasks. While the model may understand the general intent of the instruction, the generated outputs may not fully satisfy all aspects of the requested task. For example, in translation tasks, the model might incorporate some elements of the target language but fail to produce a complete and accurate translation. Besides, our current work focuses primarily on simple, single-task instructions like translation or summarization. In future, we plan to investigate how to extend this approach to handle more sophisticated instruction types, such as multi-step reasoning tasks or instructions that combine multiple objectives. Additionally, our experiments were conducted using models from the Gemma and Llama two LLM families. In the future, we plan to extend this analysis to a more diverse set of language model architectures and families to validate the generality of our findings.

References

- Andy Arditi, Oscar Obeso, Aaquib Syed, Daniel Paleka, Nina Panickssery, Wes Gurnee, and Neel Nanda. 2024. Refusal in language models is mediated by a single direction. *arXiv preprint arXiv:2406.11717*.
- Yonatan Belinkov. 2022. Probing classifiers: Promises, shortcomings, and advances. *Computational Linguistics*, 48(1):207–219.
- Trenton Bricken, Adly Templeton, Joshua Batson, Brian Chen, Adam Jermy, Tom Conerly, Nicholas L Turner, Cem Anil, Carson Denison, Amanda Askell, Robert Lasenby, Yifan Wu, Shauna Kravec, Nicholas Schiefer, Tim Maxwell, Nicholas Joseph, Alex Tamkin, Karina Nguyen, Brayden McLean, Josiah E Burke, Tristan Hume, Shan Carter, Tom Henighan, and Chris Olah. 2023. [Towards monosemanticity: Decomposing language models with dictionary learning](#).
- Hyung Won Chung, Le Hou, Shayne Longpre, Barret Zoph, Yi Tay, William Fedus, Yunxuan Li, Xuezhi Wang, Mostafa Dehghani, Siddhartha Brahma, Albert Webson, Shixiang Shane Gu, Zhuyun Dai, Mirac Suzgun, Xinyun Chen, Aakanksha Chowdhery, Alex Castro-Ros, Marie Pellat, Kevin Robinson, Dasha Valter, Sharan Narang, Gaurav Mishra, Adams Yu, Vincent Zhao, Yanping Huang, Andrew Dai, Hongkun Yu, Slav Petrov, Ed H. Chi, Jeff Dean, Jacob Devlin, Adam Roberts, Denny Zhou, Quoc V. Le, and Jason Wei. 2024. [Scaling instruction-finetuned language models](#). *Journal of Machine Learning Research (JMLR)*, 25(70):1–53.
- Alexis Conneau, Ruty Rinott, Guillaume Lample, Adina Williams, Samuel R. Bowman, Holger Schwenk, and Veselin Stoyanov. 2018. Xnli: Evaluating cross-lingual sentence representations. In *Proceedings of the 2018 Conference on Empirical Methods in Natural Language Processing*. Association for Computational Linguistics.
- Javier Ferrando, Oscar Balcells Obeso, Senthoran Rajamanoharan, and Neel Nanda. 2025. [Do i know this entity? knowledge awareness and hallucinations in language models](#). In *The Thirteenth International Conference on Learning Representations*.
- Leo Gao, Tom Dupré la Tour, Henk Tillman, Gabriel Goh, Rajan Troll, Alec Radford, Ilya Sutskever, Jan Leike, and Jeffrey Wu. 2024. Scaling and evaluating sparse autoencoders. *arXiv preprint arXiv:2406.04093*.
- Zhengfu He, Wentao Shu, Xuyang Ge, Lingjie Chen, Junxuan Wang, Yunhua Zhou, Frances Liu, Qipeng Guo, Xuanjing Huang, Zuxuan Wu, et al. 2024. Llama scope: Extracting millions of features from llama-3.1-8b with sparse autoencoders. *arXiv preprint arXiv:2410.20526*.
- John Hewitt, Nelson F Liu, Percy Liang, and Christopher D Manning. 2024. Instruction following without instruction tuning. *arXiv preprint arXiv:2409.14254*.
- Ole Jorgensen, Dylan Cope, Nandi Schoots, and Murray Shanahan. 2024. Improving activation steering in language models with mean-centring. In *Responsible Language Models Workshop at AAAI-24*.
- Been Kim, Martin Wattenberg, Justin Gilmer, Carrie Cai, James Wexler, Fernanda Viégas, et al. 2018. Interpretability beyond feature attribution: Quantitative testing with concept activation vectors (tcav). In *International conference on machine learning*, pages 2668–2677. PMLR.
- Connor Kissane, Robert Krzyzanowski, Joseph Isaac Bloom, Arthur Conmy, and Neel Nanda. 2024. Interpreting attention layer outputs with sparse autoencoders. In *ICML 2024 Workshop on Mechanistic Interpretability*.
- Po-Nien Kung and Nanyun Peng. 2023. Do models really learn to follow instructions? an empirical study of instruction tuning. In *Proceedings of the 61st Annual Meeting of the Association for Computational Linguistics (Volume 2: Short Papers)*, pages 1317–1328.
- Kenneth Li, Tianle Liu, Naomi Bashkinsky, David Bau, Fernanda Viégas, Hanspeter Pfister, and Martin Wattenberg. 2024a. Measuring and controlling persona drift in language model dialogs. *arXiv preprint arXiv:2402.10962*.
- Kenneth Li, Oam Patel, Fernanda Viégas, Hanspeter Pfister, and Martin Wattenberg. 2024b. Inference-time intervention: Eliciting truthful answers from a language model. *Advances in Neural Information Processing Systems*, 36.

- Tom Lieberum, Senthoran Rajamanoharan, Arthur Conmy, Lewis Smith, Nicolas Sonnerat, Vikrant Varma, János Kramár, Anca Dragan, Rohin Shah, and Neel Nanda. 2024. Gemma scope: Open sparse autoencoders everywhere all at once on gemma 2. *arXiv preprint arXiv:2408.05147*.
- Johnny Lin. 2023. [Neuronpedia: Interactive reference and tooling for analyzing neural networks](#). Software available from neuronpedia.org.
- Yijin Liu, Xianfeng Zeng, Fandong Meng, and Jie Zhou. 2024. Instruction position matters in sequence generation with large language models. In *Findings of the Association for Computational Linguistics: ACL 2024*.
- Wanqin Ma, Chenyang Yang, and Christian Kästner. 2024. [\(why\) is my prompt getting worse? rethinking regression testing for evolving llm apis](#). In *Proceedings of the IEEE/ACM 3rd International Conference on AI Engineering - Software Engineering for AI, CAIN '24*, page 166–171, New York, NY, USA. Association for Computing Machinery.
- Samuel Marks and Max Tegmark. 2024. The geometry of truth: Emergent linear structure in large language model representations of true/false datasets. In *Conference on Language Modeling*.
- Bruno A. Olshausen and David J. Field. 1997. [Sparse coding with an overcomplete basis set: A strategy employed by v1?](#) *Vision Research*, 37(23):3311–3325.
- Long Ouyang, Jeffrey Wu, Xu Jiang, Diogo Almeida, Carroll Wainwright, Pamela Mishkin, Chong Zhang, Sandhini Agarwal, Katarina Slama, Alex Ray, et al. 2022. Training language models to follow instructions with human feedback. *Advances in Neural Information Processing Systems (NeurIPS)*, 35:27730–27744.
- Senthoran Rajamanoharan, Tom Lieberum, Nicolas Sonnerat, Arthur Conmy, Vikrant Varma, János Kramár, and Neel Nanda. 2024. [Jumping ahead: Improving reconstruction fidelity with jumprelu sparse autoencoders](#). *Preprint*, arXiv:2407.14435.
- Nina Rimskey, Nick Gabrieli, Julian Schulz, Meg Tong, Evan Hubinger, and Alexander Turner. 2024. Steering llama 2 via contrastive activation addition. In *Proceedings of the 62nd Annual Meeting of the Association for Computational Linguistics (Volume 1: Long Papers)*.
- Victor Sanh, Albert Webson, Colin Raffel, Stephen H Bach, Lintang Sutawika, Zaid Alyafeai, Antoine Chaffin, Arnaud Stiegler, Teven Le Scao, Arun Raja, et al. 2022. Multitask prompted training enables zero-shot task generalization. In *International Conference on Learning Representations*.
- Lee Sharkey, Dan Braun, and Beren Millidge. 2022. [Taking features out of superposition with sparse autoencoders](#).
- Alessandro Stolfo, Vidhisha Balachandran, Safoora Yousefi, Eric Horvitz, and Besmira Nushi. 2024. Improving instruction-following in language models through activation steering. *arXiv preprint arXiv:2410.12877*.
- Jiao Sun, Yufei Tian, Wangchunshu Zhou, Nan Xu, Qian Hu, Rahul Gupta, John Wieting, Nanyun Peng, and Xuezhe Ma. 2023. [Evaluating large language models on controlled generation tasks](#). In *Proceedings of the 2023 Conference on Empirical Methods in Natural Language Processing (EMNLP)*, pages 3155–3168, Singapore. Association for Computational Linguistics.
- Gemma Team, Morgane Riviere, Shreya Pathak, Pier Giuseppe Sessa, Cassidy Hardin, Surya Bhupatiraju, Léonard Hussenot, Thomas Mesnard, Bobak Shahriari, Alexandre Ramé, et al. 2024. Gemma 2: Improving open language models at a practical size. *arXiv preprint arXiv:2408.00118*.
- Curt Tigges, Oskar John Hollinsworth, Atticus Geiger, and Neel Nanda. 2023. [Linear representations of sentiment in large language models](#). *Preprint*, arXiv:2310.15154.
- Jason Wei, Maarten Bosma, Vincent Zhao, Kelvin Guu, Adams Wei Yu, Brian Lester, Nan Du, Andrew M. Dai, and Quoc V Le. 2022. [Finetuned language models are zero-shot learners](#). In *International Conference on Learning Representations (ICLR)*.
- Haiyan Zhao, Heng Zhao, Bo Shen, Ali Payani, Fan Yang, and Mengnan Du. 2025. [Beyond single concept vector: Modeling concept subspace in LLMs with gaussian distribution](#). In *The Thirteenth International Conference on Learning Representations*.
- Chunting Zhou, Pengfei Liu, Puxin Xu, Srinivasan Iyer, Jiao Sun, Yuning Mao, Xuezhe Ma, Avia Efrat, Ping Yu, Lili Yu, et al. 2024. Lima: Less is more for alignment. *Advances in Neural Information Processing Systems*, 36.
- Jeffrey Zhou, Tianjian Lu, Swaroop Mishra, Sidhartha Brahma, Sujoy Basu, Yi Luan, Denny Zhou, and Le Hou. 2023. Instruction-following evaluation for large language models. *arXiv preprint arXiv:2311.07911*.
- Andy Zou, Long Phan, Sarah Chen, James Campbell, Phillip Guo, Richard Ren, Alexander Pan, Xuwang Yin, Mantas Mazeika, Ann-Kathrin Dombrowski, Shashwat Goel, Nathaniel Li, Michael J. Byun, Zifan Wang, Alex Mallen, Steven Basart, Sanmi Koyejo, Dawn Song, Matt Fredrikson, J. Zico Kolter, and Dan Hendrycks. 2023. [Representation engineering: A top-down approach to ai transparency](#). *Preprint*, arXiv:2310.01405.

A Details of Instructions

Instruction	Description
Include Keywords	Include keyword {keyword} in your response. In your response, the keyword {keyword} should appear. Answer with keyword {keyword} in your response. 在你的回答中包含关键词 {keyword}。 Fügen Sie das Schlüsselwort {keyword} in Ihre Antwort ein. 返信の中にキーワード {keyword} を含めてください。
Extraction	Provide a summary of this text. Summarize this sentence. Give me the bullet points of the given content. 请对这段文字做一个总结。 Fassen Sie diesen Text zusammen. このテキストの要約を提供してください。
Translation (French)	Translate the sentence to French. Provide a French translation of the given text. Convert this sentence to French. 请把这个句子翻译成法语。 Übersetzen Sie den Satz ins Französische. この文を仏語に翻訳してください。
Translation (English)	Translate the sentence to English. Provide an English translation of the given text. Convert this sentence to English. 请把这个句子翻译成英语。 Übersetzen Sie den Satz ins Englische. この文を英語に翻訳してください。
Translation (Chinese)	Translate the sentence to Chinese. Provide a Chinese translation of the given text. Convert this sentence to Chinese. 请把这个句子翻译成中文。 Übersetzen Sie den Satz ins Chinesische. この文を中国語に翻訳してください。

B Related Work

In this section, we briefly summarize several research directions that are most relevant to ours.

Instruction Following in Language Models. Instruction following capabilities are crucial for improving LLM performance and ensuring safe deployment. Recent advances in instruction tuning have demonstrated significant progress through various methods (Ouyang et al., 2022; Sanh et al., 2022; Wei et al., 2022; Chung et al., 2024). However, capable models still struggle with hard-constrained tasks (Sun et al., 2023) and lengthy generations (Li et al., 2024a). Some studies find that instruction following can be improved with in-context few-shot examples (Kung and Peng, 2023), optimal instruction positions (Liu et al., 2024), carefully selected instruction-response pairs with fine-tuning (Zhou et al., 2024), and adaptations (Hewitt et al., 2024). Unfortunately, the mechanistic understanding of how LLMs internally represent and process these instructions remains limited.

Language Model Representations. A body of research have focused on studying the linear representation of concepts in representation space (Kim et al., 2018). The basic idea is to find a direction in the

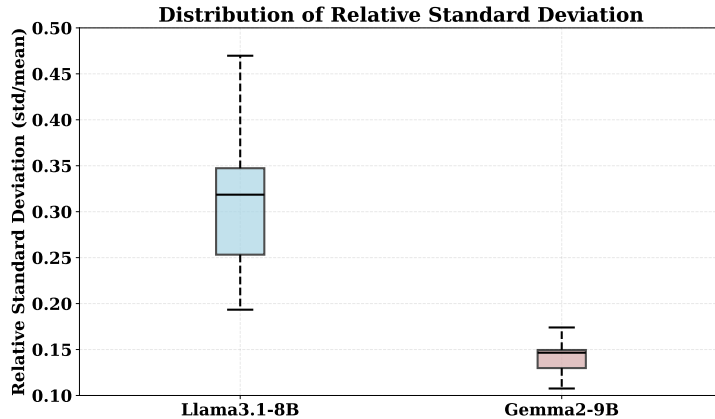


Figure 6: Visualization of steering vectors extracted from LLaMA-3.1-8B and Gemma-2-9B for French translation task. The y-axis denotes the ratio between the standard deviation and mean of feature activation strengths.

space to represent the related concept. This can be achieved using a dataset with positive and negative samples relevant to concepts. Existing approaches computing the concept vectors include probing classifiers (Belinkov, 2022), mean difference (Rimsky et al., 2024; Zou et al., 2023), mean centering (Jorgensen et al., 2024), gaussian concept subspace (Zhao et al., 2025), which provide a rich set of tools to derive concept vectors. The derived concept vectors represent various high-level concepts such as honesty (Li et al., 2024b), truthfulness (Tigges et al., 2023), harmfulness (Zou et al., 2023), and sentiments (Zhao et al., 2025).

Sparse Autoencoders. Dictionary learning is effective in disentangling features in superposition without representation space. Sparse autoencoder (SAE) offers a feasible way to map representations into a higher-dimension space and reconstruct to representation space. Various SAEs have been proposed to improve their performance such as vallina SAEs (Sharkey et al., 2022), TopK SAEs (Gao et al., 2024). Based on them, a range of sparse autoencoders (SAEs) have been trained to interpret hidden representations including Gemma Scope (Lieberum et al., 2024) and Llama Scope (He et al., 2024). These SAEs have also been used to interpret models’ representational output (Kissane et al., 2024) and understand their abilities (Ferrando et al., 2025).

Activation Steering. Recently, a body of research has utilized concept vectors to steer model behaviors during inference. Specifically, concepts vectors can be computed with diverse approaches, and these vectors are mostly effective on manipulating models generating concept-relevant text. For instance, many studies find it useful in improving truthfulness (Marks and Tegmark, 2024) and safety (Arditi et al., 2024), mitigating sycophantic and biases (Zou et al., 2023). Steering primarily operates in the residual stream following methods defined in Eq. (3), but it is worth-noting that the steering vectors can be computed from either residual stream representations or SAEs. Existing work mostly concentrates on computing with residual stream representations, which provide limited insights on what finer features contribute to the high-level concept vector. This coarse approach could further limit our deeper understanding on more complicated vectors such as instructions. In our work, we aim to bridge this gap by studying instruction vectors with SAEs to uncover their working mechanism.

C Additional Results for Llama-3.1-8b

In our experimental setup, we employ Equation (7) to control feature activation during model steering, where μ_i denotes the pre-computed mean activation strength and s_i represents the standard deviation for feature i . The hyperparameter β controls the perturbation magnitude relative to the standard deviation. Our experiments reveal distinct robustness characteristics across different model architectures. For the Gemma-2 family models, the steering vectors maintain their effectiveness when $\beta \in [-1, 1]$, indicating robust feature representations. These models exhibit high activation strength values (μ_i) with low standard deviations (s_i), suggesting stable and consistent feature characteristics. In contrast, the Llama-3.1-8b

Table 5: Evaluation Prompt for Generated Output

Your task is to strictly evaluate whether the generated output follows the given instruction. First you should review the following components:

Original Input: {input_text}
 Instruction: {instruction}
 Generated Output: {generated_output}

Here is the evaluation criteria:

A: The generated content completely follows the instruction.
 B: Contains instruction keywords but doesn't follow the instruction completely.
 C: Completely irrelevant to the instruction Critical.

Remember:

If the Generated Output only contains repeated words or sentences, select C immediately.

DO NOT provide explanation. Provide your evaluation by selecting one option(A/B/C).

Your Answer is:

model demonstrates higher sensitivity to activation perturbations. The steering vectors remain effective only when $\beta \in [-0.1, 0.1]$, indicating a significantly narrower tolerance range. The relative standard deviations illustrated in Figure 6 quantify this distinction. This narrow tolerance range suggests that Llama-3.1-8b's feature space may possess the following characteristics: stricter boundaries between features, more discrete transitions between different instruction states, and poorer robustness to noise.

D Steering Accuracy Evaluation based on GPT-4o-mini

To evaluate generated outputs, we instruct GPT-4o-mini to rate in the following way. For each instance, we provide GPT-4o-mini with three components: the original input text, the instruction, and the model-generated output. To ensure reliable assessment, we implement a voting mechanism where GPT-4o-mini performs five independent evaluations for each instance. For each evaluation, GPT-4o-mini is prompted to assess the instruction following level by selecting whether the generated content completely follows the instruction (A), contains instruction keywords but doesn't follow the instruction (B), or is completely irrelevant to the instruction (C). The final grade is determined by majority voting among the five evaluations. In cases where there is no clear majority (e.g., when votes are split as 2-2-1), we choose the lower grade between the two options that received the most votes (C is considered lower than B, and B is lower than A). This ensures a stringent evaluation standard when the votes are divided. Thus, the *Strict Accuracy* is the ratio of A and the *Loose Accuracy* is the ratio of A + B. The prompt we use in the experiments can be found in Table 5.

E Model Scale Analysis

We explore the influence of both model scale and SAE scale, showing larger sizes always contribute to better performance. Using SAE with larger dimensions (e.g., increasing Gemma-2-2b's SAE from 16K to 65K) can effectively improve the interpretability of feature extraction. For the same prompt, Gemma-2-2b's 16K SAE is almost unable to extract interpretable features under our settings, while the 65K model performs well. For Gemma-2-9b and Llama3.1-8b models, even the SAE with minimal dimensions can extract features with good interpretability.

F More Activating Examples of Top-ranked Features

Table 6: The remaining eight features we used to construct the steering vector for Gemma2-2B SAE on the French Translation task, along with their corresponding activation examples. (The other seven features can be found in Table 1 and Table 2.) The examples are provided by Neuropedia (Lin & Bloom, 2024).

Layer25, Feature42374
Could you please translate the following sentence to French? I think "everyone" and "we" are the same in this sentence .
Layer25, Feature49454
Quote from the article below : Variable names are case - sensitive. With pure mind and internal contemplation there is no need for...
Layer25, Feature54902
The incredible spe ta culo de la vida , the incredible spe ta culo de la muerte! This is a continuation of the precedent the band established with Re...
Layer25, Feature55427
Whatever the modifier may be , both sentences are discussing... I can make no distinction between the two lsentences at issue...
Layer25, Feature6201
Furthermore, figure has a plethora of other senses , evinced by the dictionary entry linked above. The meaning and nuance of this phrase can be quite different depending on the context .
Layer25, Feature17780
How to convert the text into Hyperlinks? Thanks in advance! Hi Jimmy, I don't have your grandfather Birl listed in my files...
Layer25, Feature22091
She can't focus sufficiently to utter complete sentences without needing to stop and reflect. He speaks in a Hiroshima accent and often ends his sentences with " garu" and " ja".
Layer25, Feature59061
Helderberg is a Dutch name meaning "clear mountrain". Kaila - Altered form of English Kaylay , meaning "slender".

G Examples of Instruction Following Tasks with Steering Vectors

An example of French-Translation Task (Loose Instruction Following)

Prompt: They got divorced because the wife found out that the husband had betrayed her.

Output: French Translation: Please translate the translation into French. Translation does not translate properly in its current format, we need to rewrite it. Please rewrite the translation into French.

An example of Include Keyword Task (Failed to follow Instruction)

Prompt: Chapter 6 examines the availability of resources necessary for the installation of SO₂, NO_X, and mercury control retrofit technologies for the timing and emission reductions proposed under the Clear Skies Act.

Output: Please tell me what you think is the meaning of the passage, and can you clarify the meaning of “Clear Skies Act”?

An example of Include Keyword Task (Loose Instruction Following)

Prompt: Естественный отбор занимает у миллионера yachters..

Output: To include Sunday in text, please provide more information.

An example of French-Translation Task (Failed to follow Instruction)

Prompt: Nefes kesen gösterir biri, Çin Mahallesi ' nin batı yakasında jılan bandar ' da bulunan Sri Mahamariamman Hindu Tapınağı ' nda Kwong Siew Derneği Tapınağı ' ndan kısa bir süre sonra geliyor.

Output: Translation translation Translation Translation Translation Translation Translation Translation Translation Translation Translation Translation

An example of Summarization Task (Strict Instruction Following)

Prompt: 相对较少的工人支持更多退休人员，政府鼓励退休人员工作，政府支持退休人员的经济发展，提供技能开发课程以及培训帮助退休人员回到工作岗位。

Output: The government encourages retirees to work and supports their economic development by providing skills training and courses to help them re-enter the job market.

An example of Summarization Task (Loose Instruction Following)

Prompt: So I'm up here you know nights and weekends you know working on the little PC on the PC up here you know typing stuff so I can see where it would be a great advantage to have one at home you know if you were going to school.

Output: Let me break down this sentence and give you a summary.

An example of Summarization Task (Failed to follow Instruction)

Prompt: With its economy in disarray, the government introduced a limited number of capitalist measures while maintaining a firm political grip.

Output: This was a response to its citizens' increasing demand for a more m oriented system. The phrase “limited number of capitalist measures” implies a combination of both traditional and capitalist mechanisms that would not completely free the economy from state control.

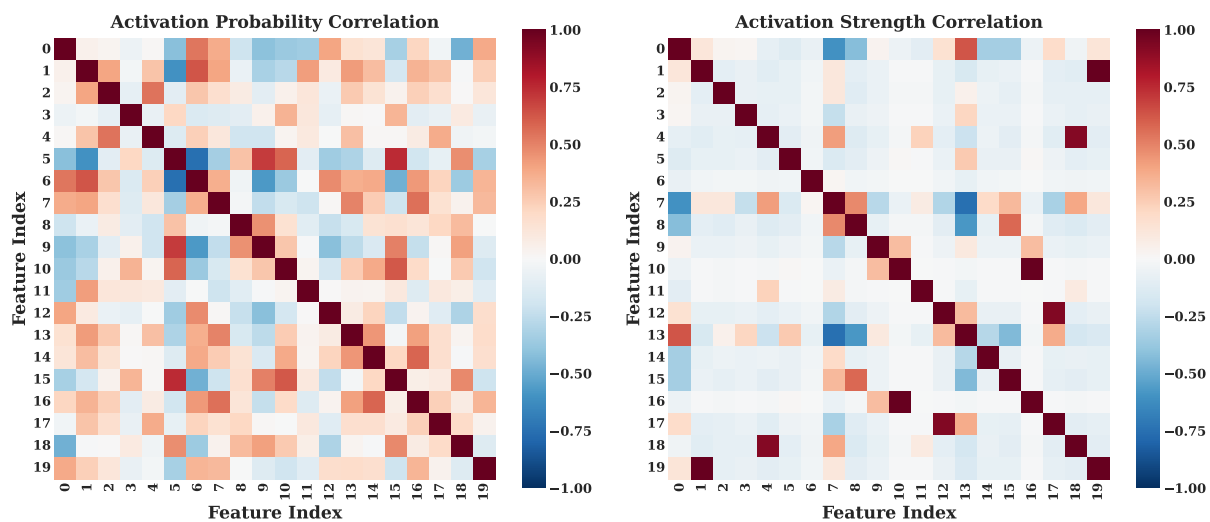
H Extracted Features Correlation Visualization and Analysis

In Section 4.5, we explored how instruction placement (before or after the original prompt) affects model behavior. To further understand how the model encodes and processes instructions in different positions, we present visualization analysis using feature correlation heatmaps. Figure 7 to Figure 11 show the feature correlations of Gemma-2-2b model across five different tasks.

Taking Figure 7 as an example, the visualization is divided into Pre-Instruction and Post-Instruction modes. Each part contains two 20×20 heatmap matrices showing Activation Probability and Activation Strength correlations respectively. The heatmaps use a red-blue color scheme, where dark red indicates strong positive correlation (1.0), dark blue indicates strong negative correlation (-1.0), and light or white areas indicate correlations close to 0. The axes range from 0 to 19, representing the top 20 SAE latent features.

Our analysis reveals distinct differences between the two instruction placement modes. The Pre-Instruction mode shows dispersed correlations with predominantly light colors outside the diagonal, indicating stronger feature independence. In contrast, the Post-Instruction mode exhibits more pronounced red and blue areas, demonstrating enhanced feature correlations and a more tightly connected feature network. This finding aligns with our key conclusion that effective instruction following requires precise combinations of multiple latent features. The stronger feature correlations in Post-Instruction mode confirm that single-feature manipulation is insufficient for reliable control. This insight into feature cooperation supports the effectiveness of our proposed steering technique based on precisely calibrated weights across multiple features.

Pre-Instruction Feature Correlations



Post-Instruction Feature Correlations

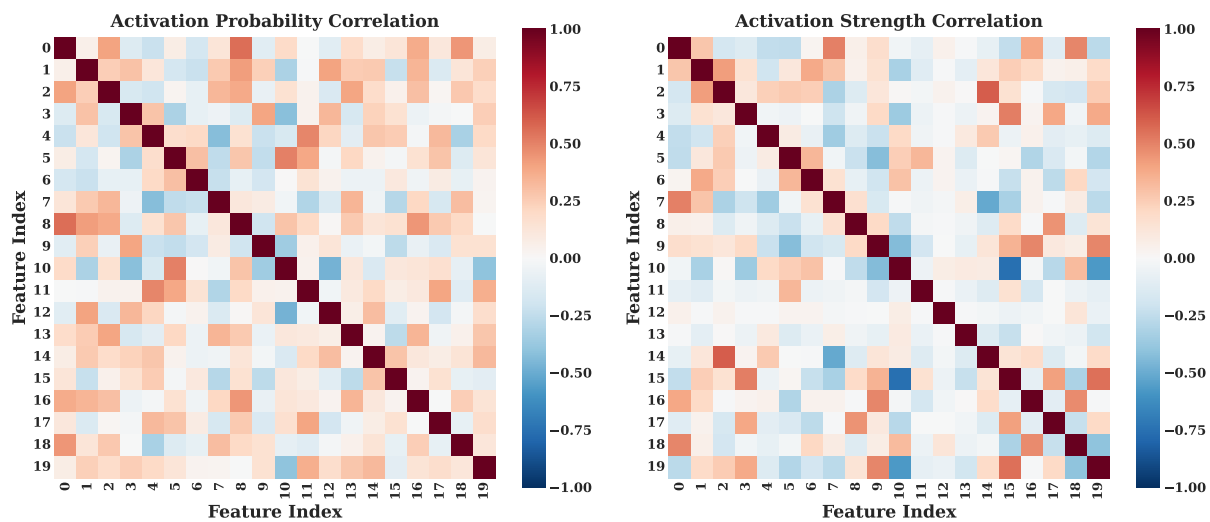
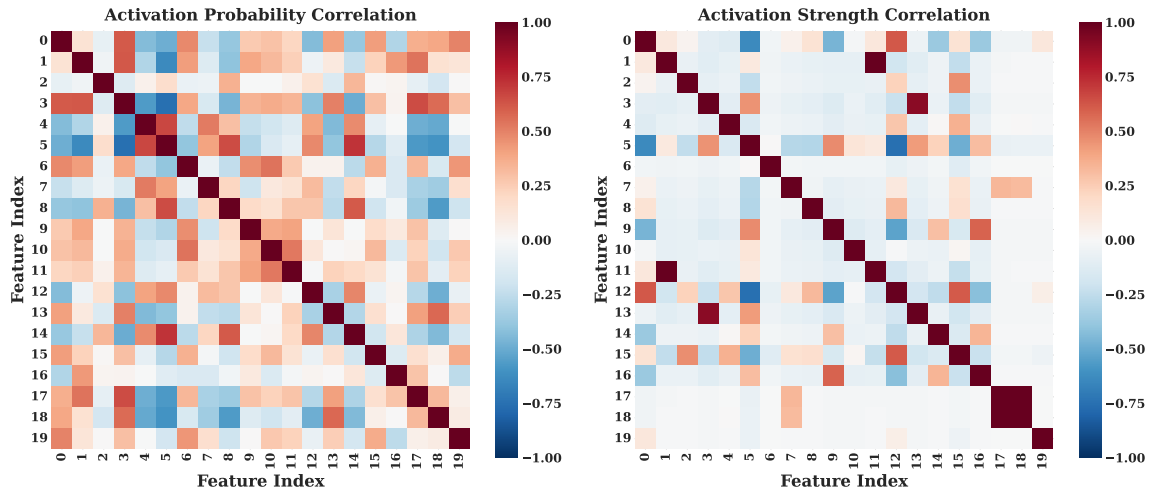


Figure 7: Heatmaps for Keyword Task.

Pre-Instruction Feature Correlations



Post-Instruction Feature Correlations

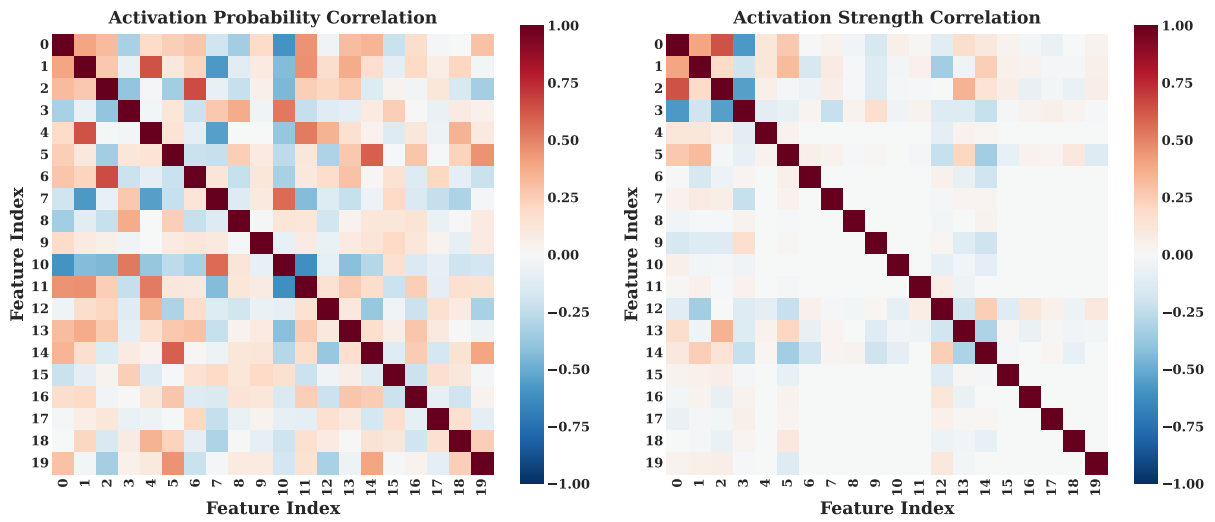
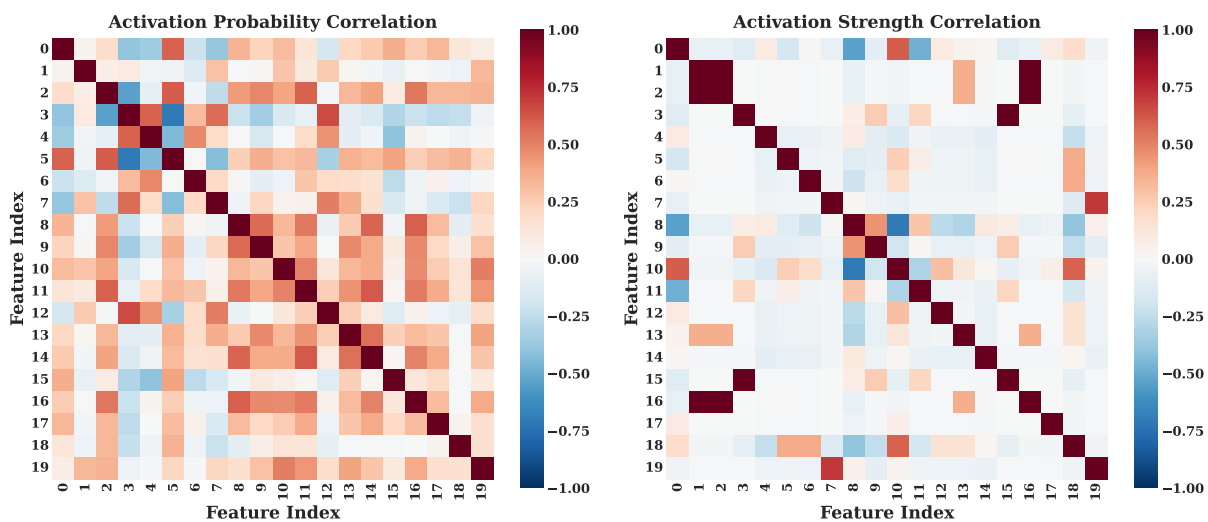


Figure 8: Heatmaps for Summarization Task.

Pre-Instruction Feature Correlations



Post-Instruction Feature Correlations

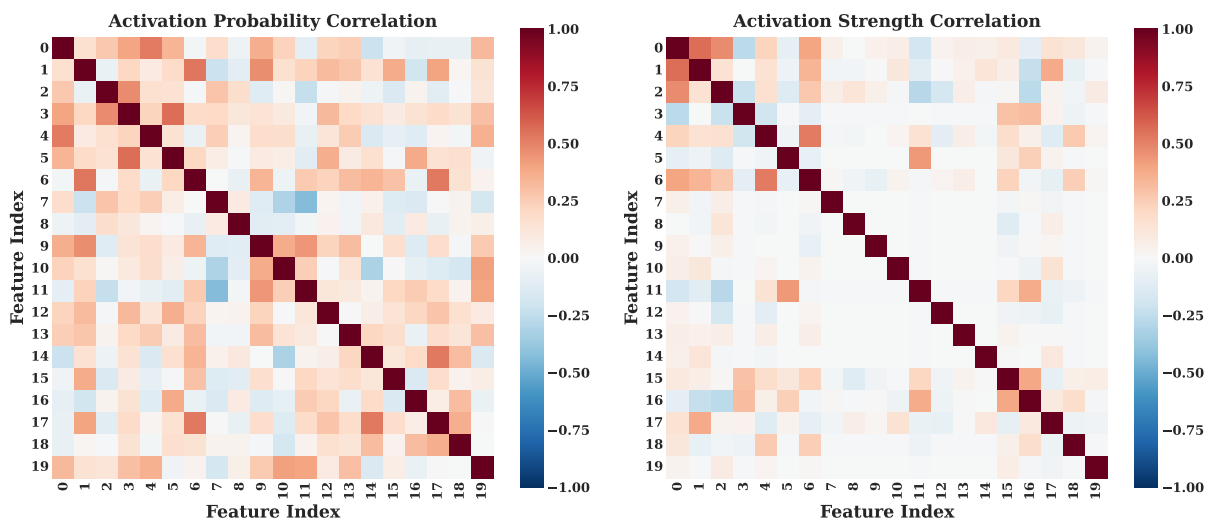
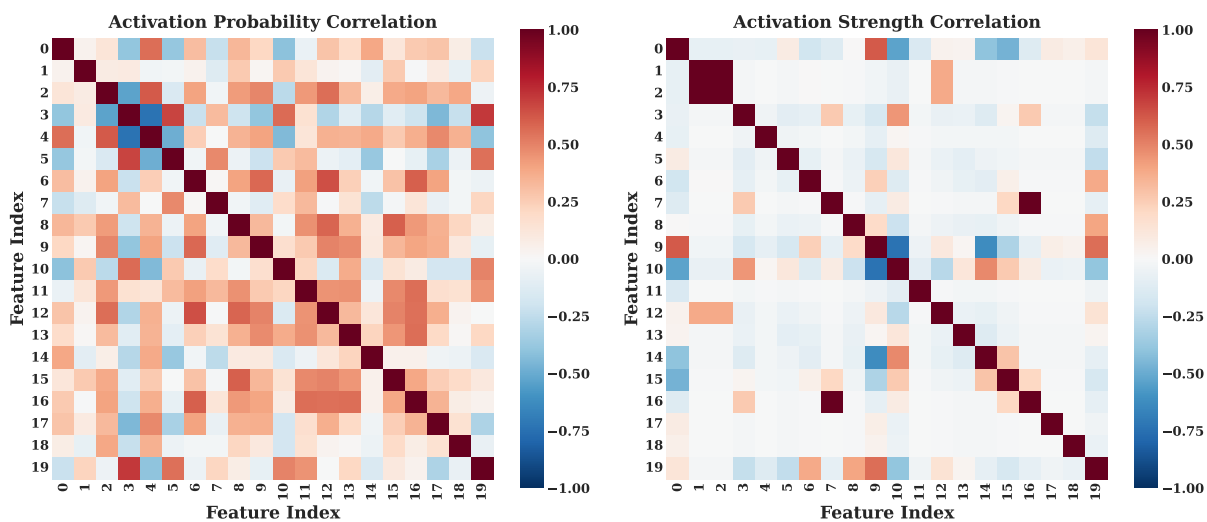


Figure 9: Heatmaps for Translation(English) Task.

Pre-Instruction Feature Correlations



Post-Instruction Feature Correlations

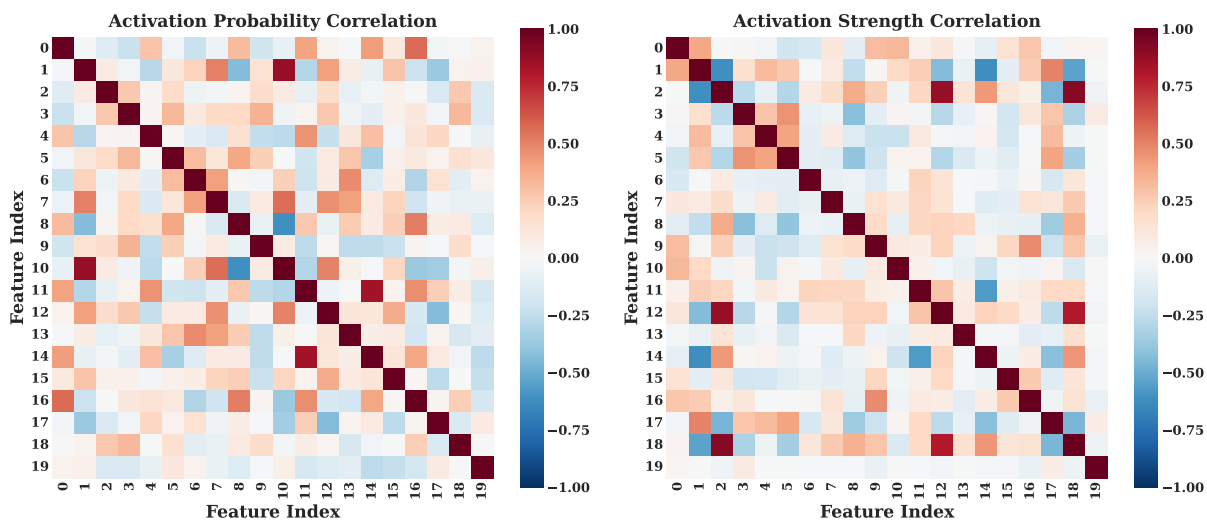
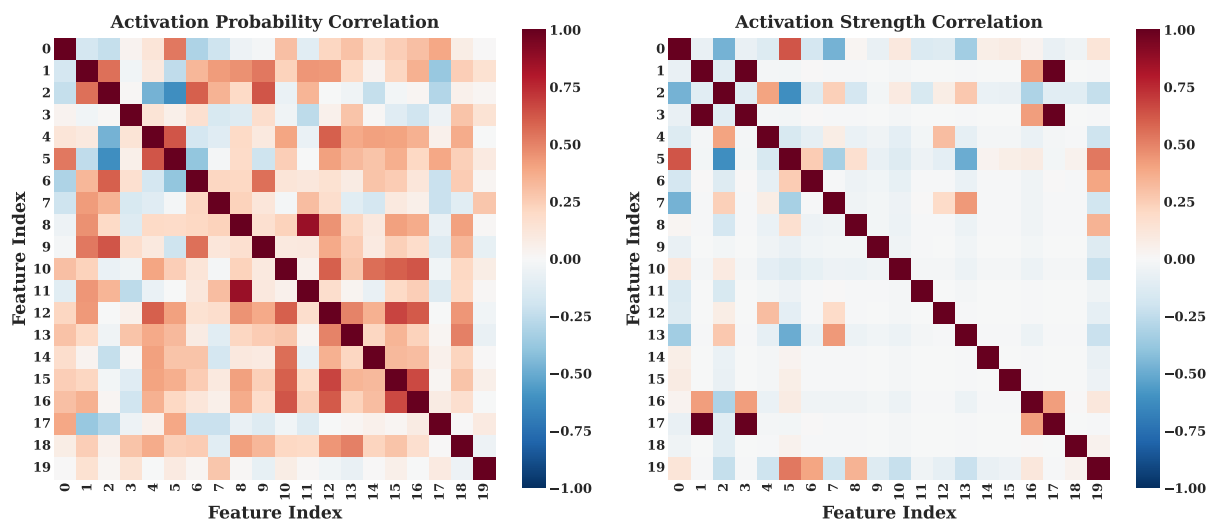


Figure 10: Heatmaps for Translation(French) Task.

Pre-Instruction Feature Correlations



Post-Instruction Feature Correlations

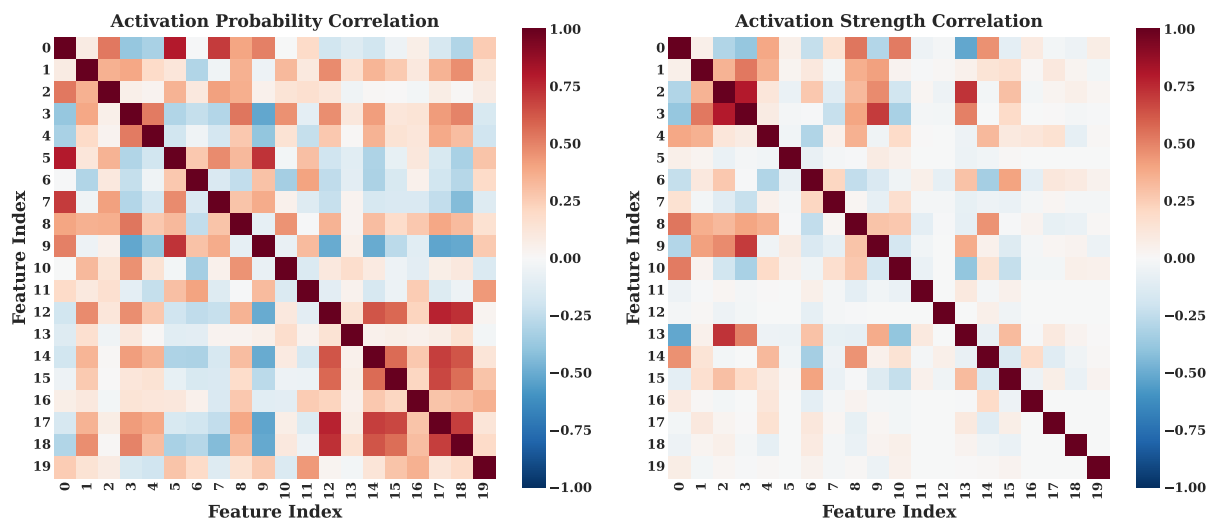


Figure 11: Heatmaps for Translation(Chinese) Task.